

# DAP5 Promotes Cap-Independent Translation of Bcl-2 and CDK1 to Facilitate Cell Survival during Mitosis

Lea Marash,<sup>1,3</sup> Noa Liberman,<sup>1,3</sup> Sivan Henis-Korenblit,<sup>1,4</sup> Gilad Sivan,<sup>2</sup> Eran Reem,<sup>1</sup> Orna Elroy-Stein,<sup>2</sup> and Adi Kimchi<sup>1,\*</sup>

<sup>1</sup>Department of Molecular Genetics, Weizmann Institute of Science, Rehovot 76100, Israel

<sup>2</sup>Department of Cell Research and Immunology, George S. Wise Faculty of Life Sciences, Tel Aviv University, Tel Aviv 69978, Israel

<sup>3</sup>These authors contributed equally to this work.

<sup>4</sup>Present address: Department of Biochemistry and Biophysics, University of California, San Francisco, San Francisco, CA 94158-2517, USA.

\*Correspondence: adi.kimchi@weizmann.ac.il

DOI 10.1016/j.molcel.2008.03.018

## SUMMARY

DAP5 is an eIF4G protein previously implicated in mediating cap-independent translation in response to cellular stresses. Here we report that DAP5 is crucial for continuous cell survival in nonstressed cells. The knockdown of endogenous DAP5 induced M phase-specific caspase-dependent apoptosis. Bcl-2 and CDK1 were identified by two independent screens as DAP5 translation targets. Notably, the activity of the Bcl-2 IRES was reduced in DAP5 knockdown cells and a selective shift of Bcl-2 mRNA toward light polysomal fractions was detected. Furthermore, a functional IRES was identified in the 5'UTR of CDK1. At the cellular level, attenuated translation of CDK1 by DAP5 knockdown decreased the phosphorylation of its M phase substrates. Ectopic expression of Bcl-2 or CDK1 proteins partially reduced the extent of caspase activation caused by DAP5 knockdown. Thus, DAP5 is necessary for maintaining cell survival during mitosis by promoting cap-independent translation of at least two prosurvival proteins.

## INTRODUCTION

Initiation of protein synthesis in the eukaryotic cell proceeds by two major mechanisms: cap dependent, which involves the assembly of the preinitiation complex at the 5' cap m<sup>7</sup>GpppX structure in the mRNA; and cap independent, which enables recruitment of the ribosome directly to the mRNA. The cap-dependent mode of initiation involves formation of the eIF4F complex, which consists of three subunits, eIF4A, eIF4E, and eIF4G; the latter acts as a scaffold to bridge between eIF4E and eIF4A (reviewed in Prevot et al., 2003). The second mode of initiation requires the presence of an internal ribosome entry site (IRES) element, a functional secondary structure within the mRNA's 5'UTR, which by directly interacting with the translation machinery enables initiation of translation independently of the 5' cap structure. Several dozen eukaryotic mRNAs that possess IRES elements within their 5'UTR, in addition to the cap structure,

have already been described. Many of these mRNAs encode proteins involved in growth control and cell-cycle progression, as well as programmed cell death. The cap-dependent mechanism of initiation is frequently blocked by induction of various cellular stresses. The uniqueness of the IRES-driven mode of protein translation is in its ability to proceed under conditions in which cap-dependent translation is inhibited (reviewed in Jackson, 2005; Prevot et al., 2003; Spriggs et al., 2005; Elroy-Stein and Merrick, 2007).

DAP5 (also called p97 or NAT1) is a member of the eIF4G protein family identified and cloned simultaneously by four independent studies (Imataka et al., 1997; Levy-Strumpf et al., 1997; Marash and Kimchi, 2005; Shaughnessy et al., 1997; Yamanaka et al., 1997). In our laboratory it was isolated in a genetic screen aimed at identifying prodeath genes essential for IFN- $\gamma$ -induced cell death (Levy-Strumpf et al., 1997). The homology of DAP5 to eIF4GI and eIF4GII is restricted to the central segment of eIF4GI/II, which corresponds to the eIF4A and eIF3 binding region. Thus DAP5 lacks the eIF4E binding site required for the interaction with the cap structure. This raised the hypothesis that DAP5 may drive cap-independent translation. The latter was subsequently confirmed by several research lines showing that DAP5, and in particular its caspase-cleaved DAP5/p86 isoform, regulates IRES-driven translation of various mRNAs such as c-Myc, Apaf-1, XIAP, and c-IAP1/HIAP2 in cells exposed to different stress signals (Henis-Korenblit et al., 2002; Lewis et al., 2008; Nevins et al., 2003; Warnakulasuriyarachchi et al., 2004). Work done in cell-free systems confirmed that bacterially produced DAP5 promotes the IRES-driven translation of these four mRNAs (Hundsdoerfer et al., 2005). In addition, it was shown that the 5'UTR of the DAP5 mRNA itself fulfills the set of functional requirements that define an IRES element, and that DAP5 protein is capable of supporting translation from its own IRES (Henis-Korenblit et al., 2000). In this context it was shown that the DAP5 IRES is preferentially utilized during different stress conditions such as apoptosis or ER stress, thus creating a positive autoregulatory loop in which DAP5 protein itself is responsible for its sustained translation under conditions where cap-dependent translation is compromised (Henis-Korenblit et al., 2000; Lewis et al., 2008).

Developmental studies on *DAP5*<sup>-/-</sup> mice suggested that this protein may also possess important functions without applying

external death-promoting or other stress signals on cells. It was found that *DAP5*<sup>-/-</sup> mice display early embryonic lethality, and *DAP5*-deficient embryonic stem cells fail to differentiate in cell culture, signifying a critical role in development (Yamanaka et al., 2000). Similarly, it has been recently reported that the knockdown of the zebrafish *DAP5* orthologs led to impaired mesoderm formation and early embryonic lethality (Nousch et al., 2007). In addition, loss-of-function mutations of *DAP5* in *Drosophila* showed abnormalities in embryonic germband extension and in metamorphosis (Yoshikane et al., 2007). Interestingly, in proliferating unstressed human cell lines it has been reported that DAP5 protein is found associated with polysomes (Lee and McCormick, 2006; Nousch et al., 2007). Yet the main issue regarding the ability of DAP5 to regulate exclusively cap-independent translation in unstressed cells, and the identity of potential mRNAs that may be selectively regulated by DAP5 in these cellular settings have not been addressed.

In the present study, we report that knockdown of the endogenous DAP5 protein by RNA interference in unstressed cell cultures induces substantial apoptotic cell death during mitosis. We propose that the death of DAP5 knockdown cells is a consequence of attenuated cap-independent translation of proteins, two of which were identified here as DAP5 translation targets: Bcl-2 and CDK1. The effect on translation initiation is selective, as no significant differences on the overall polysomal profile were detected and cap-dependent translation was not inhibited in DAP5 knockdown cells. Thus, DAP5 has a rate-limiting role in mediating cap-independent translation in unstressed cells, thereby promoting cell survival.

## RESULTS

### RNAi-Mediated Knockdown of DAP5 Reduces Cell Viability by Inducing Apoptotic Cell Death

In an attempt to unveil the function of the endogenous DAP5 protein, expression levels of DAP5 were knocked down by means of an shRNA-targeting plasmid in HeLa cells (Figure 1A, left). The reduction in DAP5 protein steady-state levels ranged from 80% to 99% in different experiments (Figure 1A, right). Interestingly, these DAP5 knockdown cultures of HeLa cells showed a significant reduction in the number of cells 5 days following the transfection of the shRNA (Figure 1B). Further quantification indicated that the total number of viable cells dropped at this time point by a factor of 3-fold (Figure 1C, bottom). In parallel, the extent of cell death was significantly increased as reflected by the percent of trypan blue-positive cells (Figure 1C, top), implying that DAP5 protein is required for continuous cell survival. Addition of the caspase inhibitor zVAD-fmk (referred to herein as zVAD) to the culture medium of DAP5 knockdown cells protected the cells from death (Figure 1C, top) and prevented the decrease in cell number (Figure 1C, bottom). This suggested that caspase-dependent pathways may be turned on, causing apoptotic cell death. Western blot analysis confirmed the activation of caspase-3 and the cleavage of ICAD<sub>L</sub>, a caspase substrate, in DAP5 knockdown cells. In addition, both events were efficiently inhibited in the presence of zVAD (Figure 1D). The activation of caspase-dependent substrate cleavage was confirmed by use of an independent siRNA against DAP5 (Dharma-

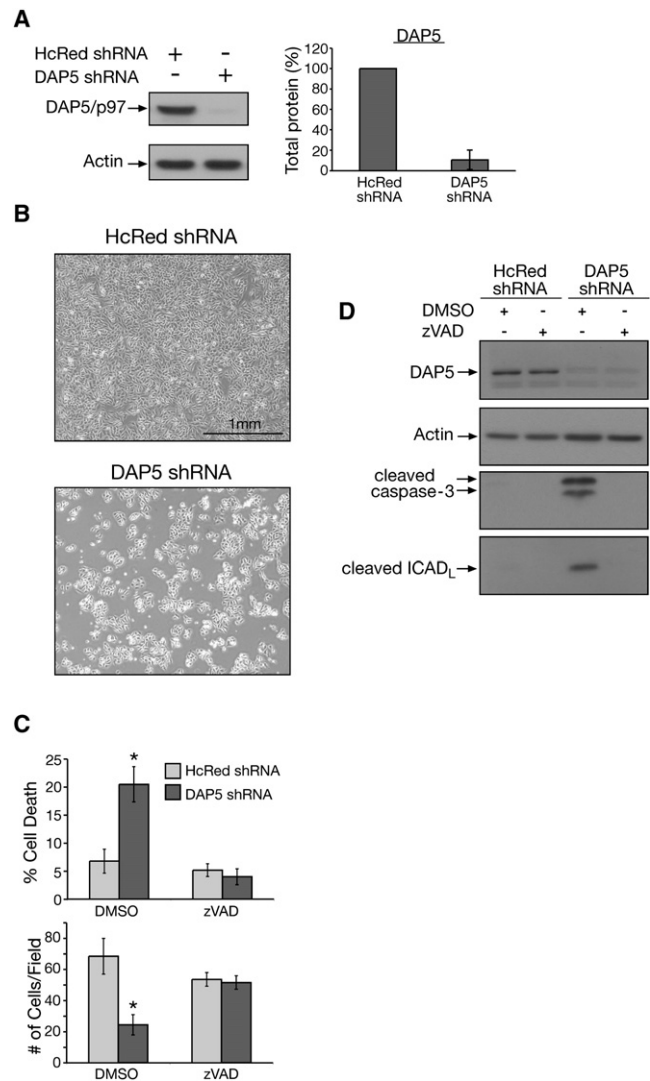


**Figure 1. DAP5 Knockdown by shRNA Affects Cell Viability and Leads to Apoptotic Cell Death**

(A) (Left) Western blot of HeLa cells transiently transfected for 5 days with shRNA against DAP5 or HcRed (control). Antibodies against DAP5 and actin (loading control) were used. (Right) Graph represents densitometry analysis of the DAP5 bands after normalization to the actin bands; the control HcRed signal was set as 100%; the values represent the mean  $\pm$  SD of ten experiments.

(B) Light micrographs of HeLa cells treated as in (A).

(C) HeLa cells transiently transfected for 5 days with indicated shRNA were treated with DMSO or zVAD for 24 hr. (Top) Graph indicates percentages of cell death as trypan blue-positive (dead) cells out of total cell number (normalized to 100%). (Bottom) Graph represents the absolute numbers of viable (trypan blue-excluding cells) per 10  $\mu$ m<sup>2</sup> field in hemicytometer. The values are presented as mean  $\pm$  SD and calculated from triplicates. Asterisks mark statistically significant results ( $p < 0.01$ ). The experiment was repeated several times with reproducible results.

(D) Western blot of HeLa cells treated as in (C), using the indicated antibodies.

con SMARTpool) to rule out possible off targets that often characterize the RNA-interference approach (see Figure S1 available online). Taken together, these observations indicate

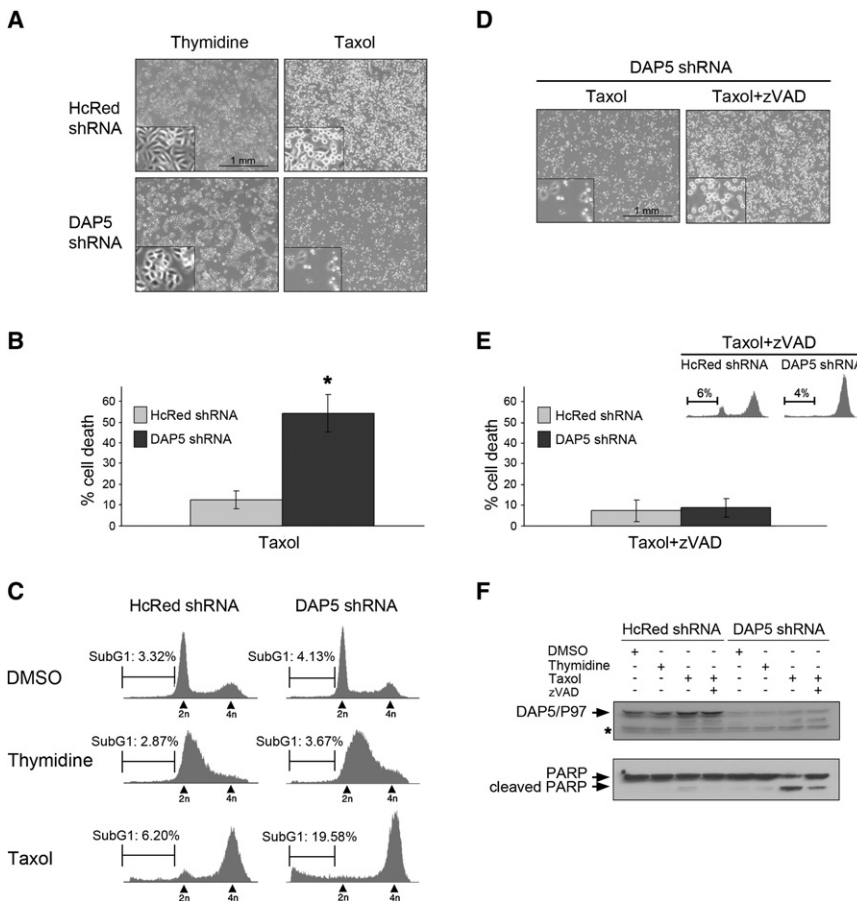


**Figure 2. DAP5 Knockdown Triggers M Phase-Specific Apoptotic Cell Death**

(A) HeLa cells transiently transfected with shRNA against DAP5 or HcRed for 5 days were plated at similar cell densities, synchronized with taxol or thymidine for 16 hr, and then visualized by light microscopy.

(B) Cells treated with taxol for 16 hr were assessed for cell death by measuring trypan blue uptake. Graph represents the mean  $\pm$  SD of triplicates. Asterisks mark statistically significant result ( $p < 0.01$ ). The experiment was repeated several times with reproducible results.

(C) Cells were treated as in (A) with taxol, thymidine, or DMSO and then stained for DNA content with propidium iodide. Histograms represent distribution of  $10^5$  cells (y axes) according to their DNA content (x axes).

(D) Cells were treated as in (A) with taxol in the absence or presence of zVAD and visualized by light microscopy.

(E) Cells were treated as in (A) with taxol and zVAD. Cell death was measured by trypan blue exclusion (graph) or by FACS analysis for sub-G1 DNA content (histograms). The values are presented as mean  $\pm$  SD and calculated from triplicates.

(F) Steady-state levels of DAP5 protein and assessment of PARP-1 cleavage, under the indicated assay conditions.

that knocking down DAP5 by RNA interference triggers caspase activation and induces apoptotic cell death.

### The Apoptotic Cell Death Induced by DAP5 Knockdown Occurs in the M Phase of the Cell Cycle

The observation that DAP5 depletion leads to apoptotic cell death, without the addition of an external trigger to the cell culture, prompted a more detailed analysis of this phenotype. To elucidate at which stage of the cell cycle DAP5 depletion had the most harmful effect on cell viability, DAP5 knockdown or control HeLa cells cultured at the same initial cell densities were arrested either at S phase by incubation with thymidine, or at M phase upon incubation with taxol (a microtubule-stabilizing agent that arrests cells at the boundary between prophase and metaphase). Notably, knockdown of DAP5 had a prominent effect on the viability of taxol-treated cells. The high extent of cell death in DAP5-depleted taxol-treated cell cultures was evident by microscopic observations and was further quantified by staining with trypan blue (Figures 2A and 2B). In addition, FACS analysis for DNA content clearly showed an elevated population with sub-G1 DNA content in taxol-treated cells with reduced DAP5 levels, corresponding to hypodiploid cells bearing fragmented DNA (Figure 2C). In contrast, DAP5 knockdown cells arrested in S phase did not show an elevation in sub-G1 cell population (Figure 2C) and displayed a less aberrant cell phenotype at this time point (Figure 2A). The addition of zVAD to DAP5 knockdown

cells protected them from cell death, inhibiting the increase in trypan blue-positive cells and in cells with fragmented DNA (Figure 2E). The drug also restored the accumulation of normal retractile mitotic cells typically observed upon taxol treatment of control cells (Figure 2D). Moreover, western blot of PARP-1, another caspase substrate, demonstrated a strong cleavage in extracts prepared from taxol-treated cells lacking DAP5 that was efficiently inhibited by the addition of zVAD (Figure 2F). The knockdown of DAP5 by a second siRNA also showed enhanced cleavage of PARP-1 and ICAD<sub>L</sub> and increased cell death in response to the taxol treatment (Figures S1 and S2). Notably, the M phase-dependent increase in caspase activation was also detected by other means of synchronization such as release from thymidine block, which leads to enrichment of mitotic cells several hours thereafter (Figure S3; see the gradual increase in ICAD<sub>L</sub> cleavage as cells proceed toward mitosis). Thus, DAP5 knockdown leads to apoptotic cell death during mitosis.

### Strategies to Identify DAP5 Translation Targets

Because DAP5 is a translation factor, the unpredicted cell-death phenotype in DAP5-depleted unstressed cells could be due to the reduction in translation of some critical DAP5 target protein(s). To enable the identification of such targets, two independent strategies to expand the repertoire of known DAP5 targets were undertaken. In the first approach, the expression of a large number of cellular proteins previously shown to be linked to cell survival was analyzed in DAP5-depleted versus control cells by western blot analysis. This was done based on the

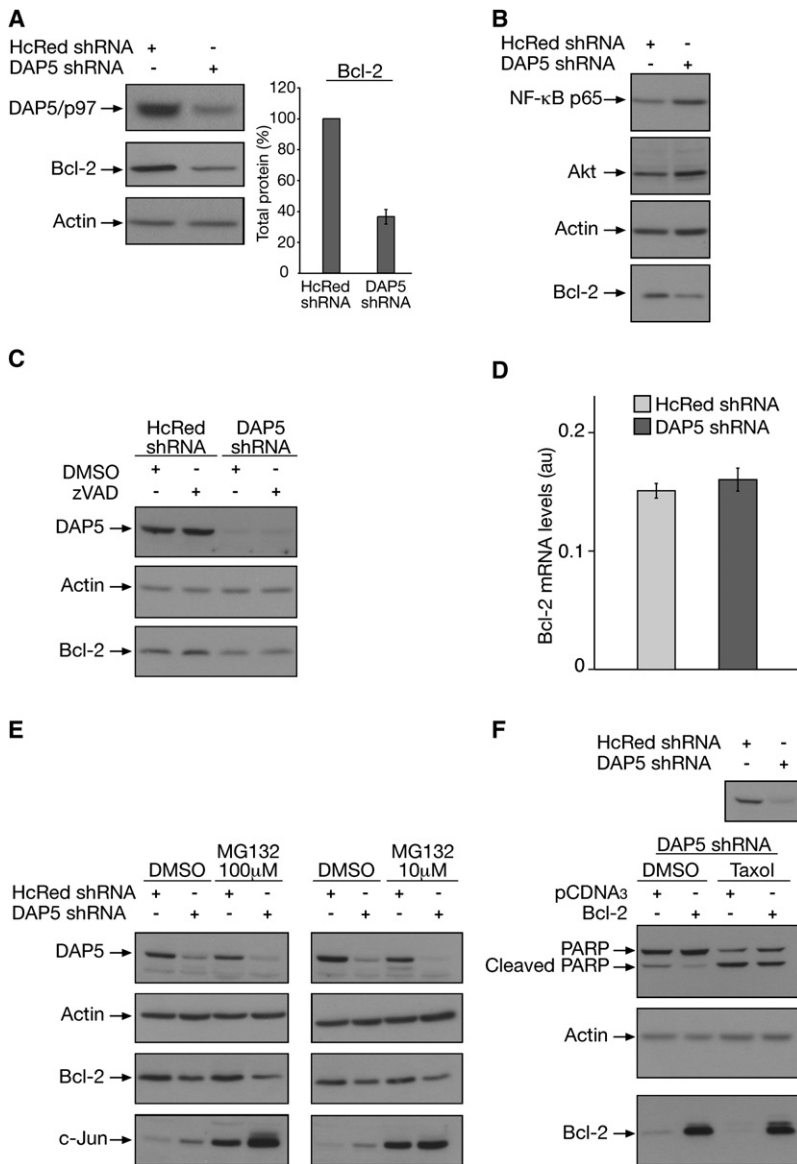


**Figure 3. Bcl-2 Is a Putative DAP5 Translation Target**

(A) HeLa cells were transfected with shRNA to DAP5 or HcRed for 5 days. Steady-state levels of DAP5, Bcl-2, and actin were assessed by immunoblotting. Graph represents densitometry analysis of the Bcl-2 bands after normalization to the actin bands; the HcRed signal was set as 100%; the values represent the mean  $\pm$  SD of six experiments.

(B) Western blot of cells treated as in (A), using the indicated antibodies.

(C) Cells depleted of DAP5 as in (A) were treated with DMSO or zVAD for 24 hr. Steady-state levels of DAP5, Bcl-2, and actin were assessed by immunoblotting.

(D) Total RNA was isolated from HeLa cells treated as in (A) and subjected to reverse transcription. Real-time PCR was performed on the cDNA samples. Relative amounts of Bcl-2 mRNA in each sample normalized to HPRT mRNA are presented as the mean  $\pm$  SD of triplicates. The experiment was repeated three times with reproducible results.

(E) Cells depleted of DAP5 as in (A) were treated for 16 hr with 10  $\mu$ M MG132 (right) or for 6 hr with 100  $\mu$ M MG132 (left). Steady-state levels of the indicated proteins were measured by immunoblotting.

(F) HeLa cells were cotransfected with DAP5 shRNA and pCDNA3 plasmid or Bcl-2 plasmid for 5 days. Cells were then treated with DMSO or taxol for 16 hr. (Top) Representative western blot of DAP5 decrease in this experiment. (Bottom) Western blot of PARP-1, actin, and Bcl-2. The rescue experiment was repeated several times with reproducible results.

assumption that modifications in translational control have to be reflected, at least partly, by changes in the steady-state protein levels of the putative target(s). In parallel, an unbiased search for mRNAs that physically interact, directly or indirectly, with DAP5 protein was performed using cDNA membrane array methodology.

### Bcl-2 Is a Putative DAP5 Target

In the first screen, we found that DAP5 depletion by RNA interference had a most striking effect on the expression of the antiapoptotic oncogene Bcl-2. The steady-state levels of endogenous Bcl-2 protein were significantly reduced in DAP5 knockdown cells, as compared to the control cells (Figure 3A). This reduction became evident 5 days following transfection with the shRNA construct against DAP5, when DAP5 depletion reaches maximal efficiency. While the reductions in the steady-state levels of Bcl-2 were evident, the steady-state levels of other

tested prosurvival proteins, Akt and NF- $\kappa$ B p65, did not change or even increased (Figure 3B). The selective reduction in Bcl-2 protein levels was confirmed by the use of an independent siRNA against DAP5 (Figure S4). Furthermore, the reduction in the steady-state levels of Bcl-2 persisted in the presence of zVAD, thus excluding possible secondary effects resulting from cell death (Figure 3C and Figure S5). Measurement of Bcl-2 mRNA levels by real-time PCR revealed equal levels of expression in cells transfected with control or DAP5 shRNA vectors (Figure 3D). In addition, the decrease in Bcl-2 protein expression was not affected by treatment with the proteasome inhibitor MG132 (Figure 3E; note that two different protocols were used, both showing the strong accumulation of the short-lived c-Jun protein, which is known to be degraded by the proteasome, indicating that the proteasome was effectively inhibited in these experiments). Taken together, these data suggest that Bcl-2 protein synthesis is regulated by DAP5.

Notably, the overexpression of Bcl-2 in DAP5 knockdown cells showed partial rescue of PARP-1 cleavage, both in non-synchronized as well as in taxol-treated cells (Figure 3F; it is shown that the ectopically expressed Bcl-2 reduced the abundance of the cleaved PARP-1 fragment from 34% to 16% in non-synchronized cells and from 74% to 55% in the taxol-treated cells). This partial yet reproducible rescue suggests that Bcl-2

is one of the critical targets of DAP5 necessary for maintaining cell viability and protecting from caspase-dependent cell death.

### Depletion of DAP5 Abrogates the IRES-Driven Translation of Bcl-2 without Affecting Cap-Dependent Translation and Global Polysomal Profile

Next we compared the polysomal profile of control and DAP5 knockdown cells by sucrose gradient fractionations. Obviously, these experiments were done in the presence of zVAD to prevent indirect effects of the caspases, activated by the DAP5 knockdown, on global protein translation. We found that knockdown of DAP5 did not affect the overall polysomal profile and there was no detectable disassembly of heavy polysomes as compared to the control cells (Figures 4A and 4B, top). The distribution of Bcl-2 mRNA was then examined by real-time PCR of each fraction, assuming that if the translation of Bcl-2 is selectively regulated by DAP5 then a redistribution of Bcl-2 mRNA from heavy polysomes to lighter polysomes upon DAP5 depletion might be observed. As an internal reference, we examined the distribution of actin mRNA as its protein product remained unchanged in the DAP5-depleted cells (Figure 3). It was found that the distribution pattern of actin mRNA on polysomes was hardly changed in the DAP5 knockdown cells (Figures 4A and 4B, upper graphs). In contrast, the distribution of Bcl-2 mRNA in DAP5 knockdown cells significantly changed toward the gradient's fractions containing lighter polysomes as compared to the control cells (Figures 4A and 4B, lower graphs; notice a shift of Bcl-2 mRNA from heavy polysomes [fractions 19–23] to lighter polysomes and subpolysomes [fractions 6–18]).

These results prompted us to examine the direct mechanism of DAP5 regulation of Bcl-2 expression. It was recently reported that the 5'UTR of Bcl-2 mRNA possesses an IRES element and that its expression is regulated at the translational level by cap-independent initiation (Sherrill et al., 2004). Given the fact that DAP5 has a role in modulating this particular mode of translation, DAP5 may in fact regulate translation from the Bcl-2 IRES. In order to test this hypothesis, bicistronic constructs containing the Bcl-2 IRES between the two luciferase cistrons (Sherrill et al., 2004) were used in a dual-luciferase reporter assay to assess IRES activity. These constructs were introduced to the cells as capped and polyadenylated bicistronic mRNAs generated by *in vitro* transcription (Figures 4C and 4D). Relative Bcl-2 IRES activity was calculated by measuring the firefly/renilla (FLuc/RLuc) ratio of luciferase luminescence. Luciferase assay was performed 6 hr following transfection according to published protocols (Sherrill et al., 2004; Yoon et al., 2006) (the luciferase activity was maximal at 6 hr following RNA transfection and significantly declined after 24 hr [data not shown], consistent with the above mentioned reports). In several independent experiments, we found that translation from the Bcl-2 IRES was reduced by ~50% in DAP5-depleted cells, as compared to control cells. In contrast, the cap-dependent translation was not affected at all in DAP5 knockdown cells (Figure 4C, lower graphs). As a consequence, the ratio between IRES-driven translation to cap-dependent translation was significantly reduced by knocking down DAP5 protein (Figure 4C, upper graph). As expected, the hairpin structure inserted upstream of the first RLuc cistron reduced cap-dependent values to background levels, while

translation from the Bcl-2 IRES remained unchanged (Figure 4D). Using this construct, the same reduction in Bcl-2 IRES activity was observed in DAP5-depleted cells as compared to the nonperturbed control cells (Figure 4D). Taken together, it is concluded that DAP5 regulates the cap-independent translation of the Bcl-2 mRNA without affecting cap-dependent global mRNA translation.

### CDK1 Is a Putative DAP5 Target

In parallel to the first approach, we developed a systematic and unbiased method for identifying IRES-containing mRNAs by searching mRNA transcripts that interact with DAP5, either directly or indirectly. Such mRNAs are promising candidates to serve as translation targets of DAP5. The approach was based on purifying RNP complexes from cells using antibodies directed against ectopically expressed DAP5, and characterizing the coimmunoprecipitated mRNAs, after RT-PCR and subsequent amplification, by hybridization to cDNA arrays. A similar approach has been successfully applied to identify RNP complexes in the study of RNA-binding proteins, including ELAV/Hu, eIF-4E, and poly(A)-binding proteins (Keene, 2001; Tenenbaum et al., 2000, 2002). As a first step, we checked whether RNP complexes could be identified by pulling down the DAP5 protein from cell extracts. To this end, specific coimmunoprecipitation of DAP5's own mRNA was used as a proof of concept for the feasibility of the approach. We have chosen for these experiments the DAP5/p86 isoform previously shown to support cap-independent translation through IRES elements (Henis-Korenblit et al., 2002; Henis-Korenblit et al., 2000). The experiments included immunoprecipitating the Flag-tagged DAP5/p86 form in HEK293T cells with anti-Flag antibodies, and quantifying the pulled-down mRNAs by RT-PCR, using primers specific for DAP5 mRNA. The levels of amplification were compared with those from nontransfected cells. In this manner, we observed a specific interaction of DAP5 protein with the DAP5 mRNA (Figure 5A). This RNP complex precipitation approach was then expanded to identify a wider spectrum of mRNAs that interact with DAP5 protein, by hybridizing the coassociated mRNAs of Flag-DAP5/p86 immunoprecipitates (or the corresponding control immunoprecipitates from nontransfected cells) to a Panorama cDNA array composed of 200 cell-cycle- and cell death-related genes. The precipitated mRNAs were first amplified using a poly(A) tail-dependent amplification step, in order to exclude genomic DNA, and then used as templates to generate radiolabeled cDNA for hybridization, using primers corresponding to the genes represented on the arrays. Upon hybridization, the phosphorimager output of the arrays was quantified and normalized to background levels and to housekeeping genes. An increase in signal of any gene on the array in DAP5 immunoprecipitates compared to the control immunoprecipitates indicated an enhancement of the corresponding mRNA in the DAP5 RNP complex. Such analysis indicated a more than 2-fold elevation in the signal in 23%–30% of the genes represented on the array. Conversely, only 1%–3% of the genes showed more than 2-fold reduction in the signal (Figure 5B). Thus, there was a clear directionality in the results, with more genes exhibiting enhanced hybridization in the DAP5/p86 sample than in the nontransfected control sample. By comparing the results of three independent

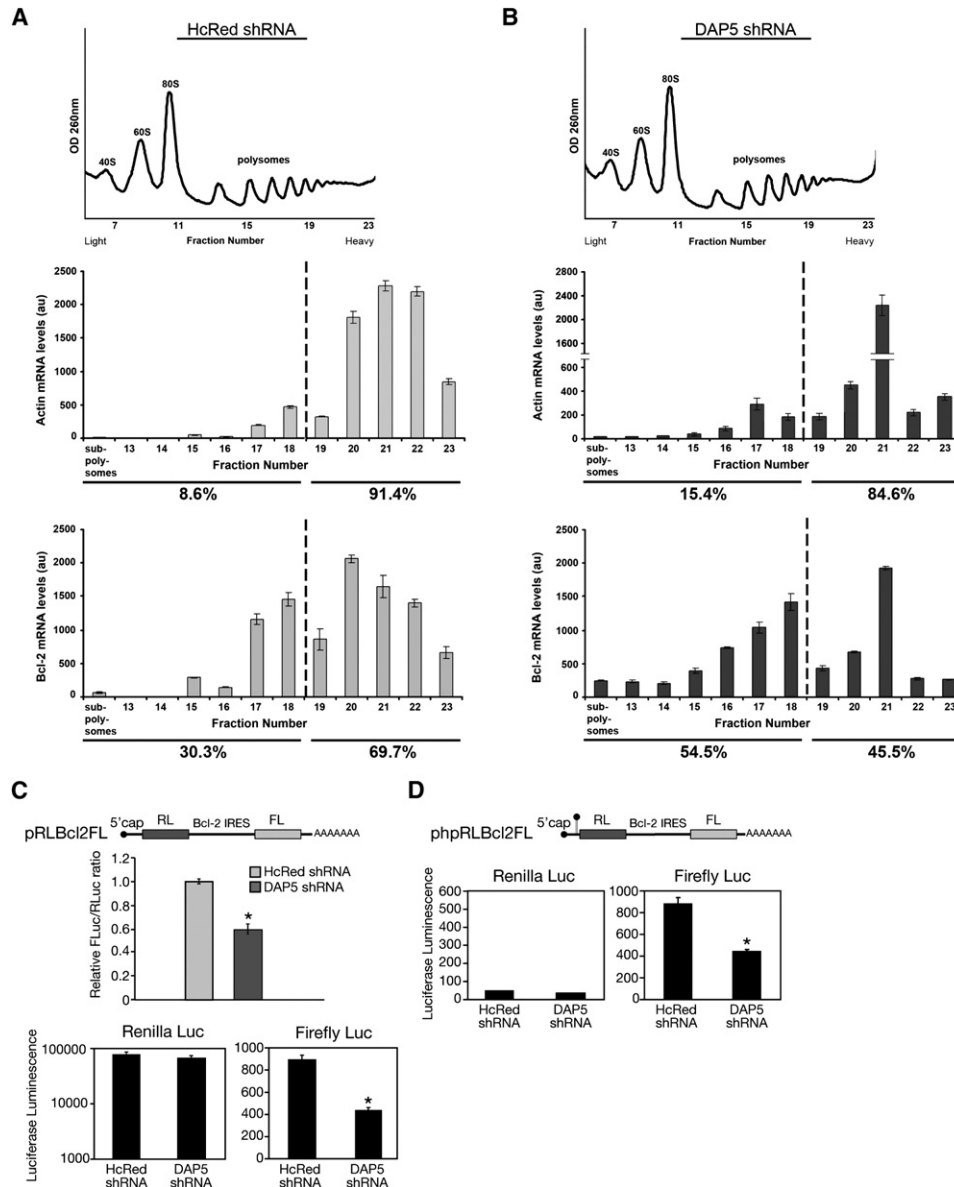


**Figure 4. DAP5 Regulates Bcl-2 Translation**

(A and B) HeLa cells transfected with shRNA to DAP5 or HcRed for 5 days were analyzed for polysomal profile. (A) (Top) Polysomal profile of HcRed shRNA-transfected cells. The 40S, 60S, 80S, and polysomes are indicated. (Bottom) Upper graph represents distribution of actin mRNA. Lower graph represents distribution of Bcl-2 mRNA. (B) (Top) Polysomal profile of DAP5 shRNA-transfected cells. The 40S, 60S, 80S, and polysomes are indicated. Upper graph represents distribution of actin mRNA. Lower graph represents distribution of Bcl-2 mRNA. Graphs represent the mean  $\pm$  SD of triplicated real-time PCR measurements of pooled fractions 6–12 indicated as subpolysomes and of each of fractions 13–23. Percent values indicate the abundance of mRNA in fractions 6–18 or 19–23 from the total amount of mRNA in fractions 6–23.

(C and D) In vitro-transcribed mRNAs from the pRLBcl2FL or phpRLBcl2FL plasmids were introduced by transfection into HeLa cells 5 days after transfection with shRNA against DAP5 or HcRed. Luciferase activity was analyzed 6 hr following the RNA transfection. (C) (Top) Schematic representation of pRLBcl2FL mRNA transcript. RL, renilla luciferase; FL, firefly luciferase. (Bottom) Upper graph represents the ratio of firefly luciferase activity to renilla luciferase activity (relative activity). The average ratio activity in the HcRed-transfected cells has been designated as 1. Lower graphs represent the absolute values reflecting renilla and firefly luciferase activity, separately, for each transcript. (D) (Top) Schematic representation of phpRLBcl2FL mRNA transcript. (Bottom) Graph representing the absolute values of renilla and firefly luciferase activity, separately. The values represent the mean  $\pm$  SD of triplicates. The experiment was repeated three times with reproducible results. Asterisks mark statistically significant results ( $p < 0.01$ ).

experiments, a group of 13 genes (6% of the total 200 genes represented on the array) were identified as positive hits increasing by more than 2-fold in all three arrays. These genes fall into path-

ways involving TNF family members, the NF- $\kappa$ B pathway, and insulin growth factor signaling. No overlap among the downregulated genes was observed.

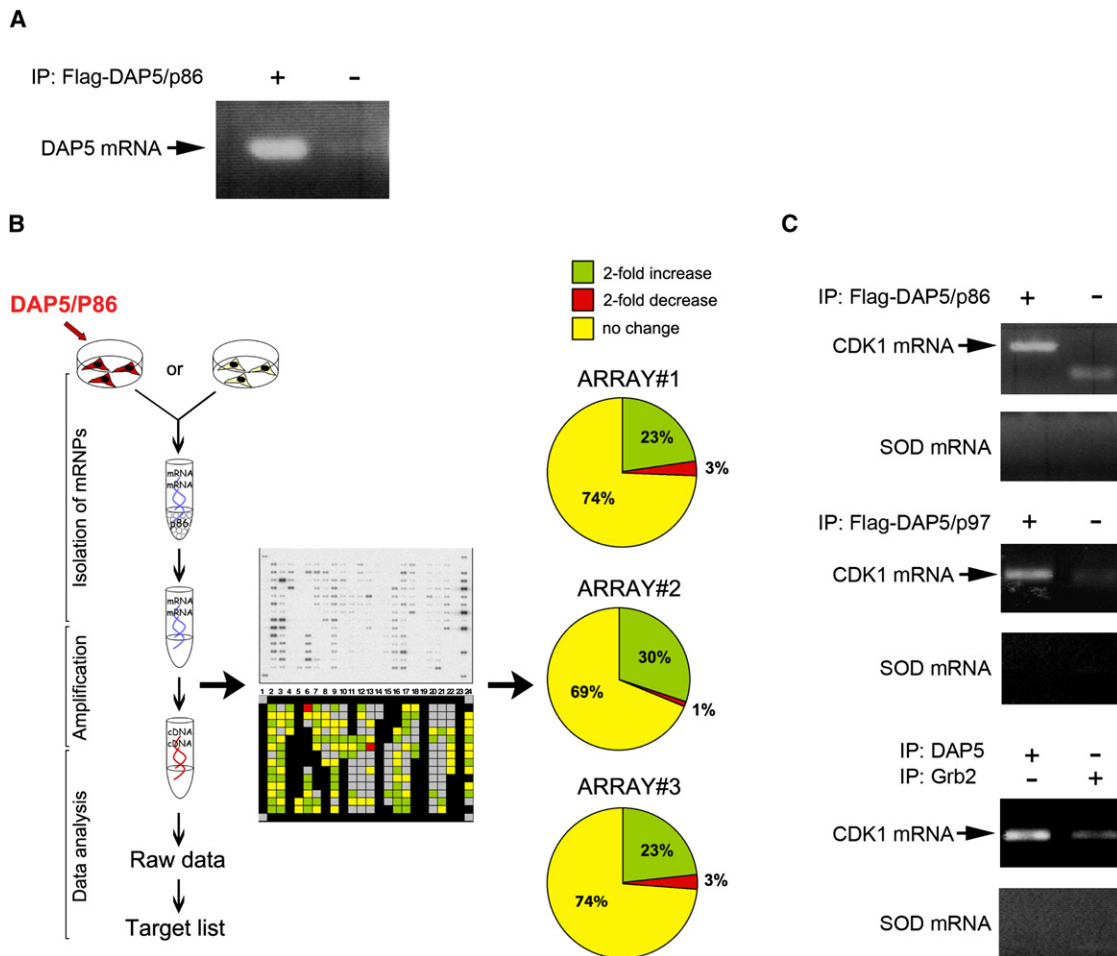


**Figure 5. CDK1 mRNA Is a Putative DAP5 Target**

(A) Total RNA was isolated from immunoprecipitates of ectopically expressed Flag-DAP5/p86 by anti-Flag antibodies and was converted to cDNA. As negative controls, immunoprecipitates of nontransfected cells were used. Detection of DAP5 mRNA in the indicated mRNP complexes was done by PCR.

(B) (Left) Schematic representation of the experimental strategy applied in the array experiments. (Right) Each pie represents results obtained from a single array experiment, in which the array hybridized to DAP5-associated cDNAs was compared to the array hybridized with template from the nontransfected control cells. Slices of the pie indicate the distribution of the genes represented on the array into three categories: those whose signal was elevated more than 2-fold compared to control (green), those with a more than 2-fold decrease in signal (red), and those exhibiting the same intensity of signal as the control (yellow).

(C) Target validation. Total RNA was isolated from the immunoprecipitates of ectopically expressed Flag-DAP5/p86 (upper panel), and ectopically expressed Flag-DAP5/p97 (middle panel) using anti-Flag antibodies. To assess possible nonspecific binding, the anti-Flag antibodies were similarly applied in nontransfected cells (right slots). In addition, RNP complexes formed by the endogenous DAP5 were generated by anti-DAP5 antibodies in nontransfected cells (lower panel). For assessing possible nonspecific binding, the same procedure was repeated with a nonrelevant antibody (i.e., anti-Grb2, right slot). The RNAs were converted to cDNAs, and detection of CDK1 mRNA was done by PCR. Specific primers for SOD mRNA that fails to bind to DAP5 protein were used as a negative control.

The most appealing putative DAP5 target identified by this screen was mRNA encoding the central mitotic kinase CDK1/p34<sup>Cdc2</sup> (referred to herein as CDK1). To validate the interaction between CDK1 mRNA and DAP5 protein, a direct assessment of CDK1 mRNA in the RNP complex with DAP5 protein was performed, using specific intron-spanning primers for CDK1 mRNA. The PCR product corresponding to CDK1 was clearly detected in DAP5, but not in the control immunoprecipitates, in several independent experiments (Figure 5C). The ectopically expressed full-length DAP5/p97 was also capable of binding the CDK1 mRNA (Figure 5C, middle panels), thus suggesting that the two DAP5 isoforms do not differ in their mRNA-binding

capability, consistent with another previous report that showed that both forms of DAP5 can similarly bind target mRNAs (Lewis et al., 2008). Importantly, the endogenous DAP5/p97 protein was also capable of specifically interacting with CDK1 mRNA under normal growth conditions, validating that this interaction occurs normally in these cells (Figure 5C, lower panel).

#### Depletion of DAP5 by shRNA Affects the Expression of CDK1 during Mitosis

Regulation of CDK1 has, to date, been described as mostly due to posttranslational modifications (Doree and Hunt, 2002; Schaffer, 1998; Stark and Taylor, 2006). Regulation at the level of

protein expression has not been addressed, and it is not known whether de novo CDK1 protein synthesis is required during mitosis. Mitosis is characterized by a switch from cap-dependent to cap-independent translation initiation. There is a general decline in protein translation, and cap-independent translation is used to maintain expression of proteins whose de novo synthesis is required for mitosis (Cornelis et al., 2000; Le Breton et al., 2005; Pyronnet et al., 2000; Pyronnet and Sonenberg, 2001; Elroy-Stein and Merrick, 2007). As a translation factor implicated in mediating cap-independent translation, DAP5 may play a role in maintaining translation of mitotic proteins. In order to determine whether CDK1 is regulated in this manner, its rate of translation during mitosis was examined. Cells were enriched in M phase by performing a double thymidine block, and allowing them to progress into mitosis following release from the block. As expected, the general rate of cellular translation, as determined by measuring the incorporation of radioactivity into TCA-precipitated material, was significantly decreased during mitosis. In contrast, CDK1 protein synthesis was selectively elevated by more than 2-fold (data not shown). To determine whether this was dependent on DAP5, the impact of DAP5 depletion on the expression of the endogenous CDK1 protein during mitosis was evaluated. Cells transfected with either shRNA to DAP5 or control shRNA were enriched in M phase by the double thymidine block. The steady-state levels of the endogenous CDK1 were significantly reduced in the DAP5-depleted cells, as compared to the control cells (Figure 6A). In order to directly measure the rate of CDK1 translation, DAP5-depleted or control cells were metabolically labeled with <sup>35</sup>S-Met, and endogenous CDK1 protein was immunoprecipitated from these cells. Taxol was used to accumulate a synchronous mitotic cell population. Consistent with the reduction in steady-state levels, de novo CDK1 translation was notably reduced in DAP5-deficient cells (Figure 6B). This reduction was also observed in the presence of zVAD, implying that it is not an indirect result of cell death in the culture (Figure 6B). Real-time PCR measurements showed no significant changes in CDK1 mRNA levels between DAP5-depleted cells and those transfected with the control shRNA, in the taxol-treated cells (Figure 6C). These data suggest that CDK1 protein translation is regulated by DAP5 during mitosis. Notably, the ectopic expression of CDK1 in DAP5 knockdown cells showed partial rescue of PARP-1 cleavage (Figure 6D; ectopically expressed CDK1 reduced the abundance of the cleaved PARP-1 fragment from 85% to 63%). This partial reproducible rescue suggests that CDK1 is another critical target of DAP5 whose reduced translation in the knockdown cells contributes to the development of the apoptotic responses in mitosis.

#### The 5'UTR of CDK1 mRNA Possesses an IRES Element

The necessity of DAP5 for CDK1 translation during mitosis suggested that its 5'UTR may contain an IRES element. In order to test for IRES activity, the entire 5'UTR of CDK1 mRNA was inserted between the two luciferase cistrons within the standard bicistronic pRLFL expression vector (Figure 6E). As with the Bcl-2 IRES described above, capped and polyadenylated mRNA was produced from pRLCDK1FL, or from empty pRLFL vector as a control, by *in vitro* transcription and was introduced into HeLa cells. Relative CDK1 IRES activity was calculated by measuring

the firefly/renilla ratio of luciferase luminescence. In several independent experiments, the 5'UTR of CDK1 mRNA was able to drive translation from the second firefly luciferase cistron, resulting in more than 3-fold increase in relative IRES activity, compared to the control (Figure 6E). Repeating these experiments on the DNA level showed similar results (Figure S6B). In addition, performing DNA experiments with the same vectors with a hairpin structure inserted before the first RLuc cistron showed reduced cap-dependent translation by 90%–95%, while translation from the CDK1 IRES still continued (Figure S6A). This suggests that the 5'UTR of CDK1 mRNA possesses an IRES element.

#### DAP5 Knockdown Cells Display a Decline in CDK1-Mediated Substrate Phosphorylation during Mitosis

The necessity of DAP5 for cell survival during mitosis suggested that DAP5 depletion and the resulting decrease in CDK1 translation may cause a prominent reduction in the phosphorylation status of CDK1 substrates. To address this issue, the level of phosphorylation of Ser/Thr Pro epitopes was measured in mitotic DAP5-depleted cells and compared to control cells, using MPM-2 antibodies. A Ser/Thr Pro sequence serves as a consensus phosphorylation site for the CDK1/cyclin B complex and is present in a wide range of cellular proteins that undergo phosphorylation at the onset of mitosis. Therefore, the degree of MPM-2 reactivity in cells, as measured by flow cytometry, reflects the overall CDK1 kinase activity in cells (O'Connor et al., 2002). As expected, MPM-2 reactivity appeared exclusively in cells with 4n DNA content (Figures 7A and 7B). Knockdown of DAP5 by shRNA, followed by treatment with taxol, led to a significant decline in the amount of MPM-2-positive cells (Figure 7A). To exclude the possibility that the reduction in the extent of Ser/Thr Pro phosphorylation during mitosis in DAP5 knockdown cells is a side effect of the massive loss of cell viability, the assay was repeated in the presence of the caspase inhibitor zVAD. Despite the fact that addition of zVAD completely restored cell viability, the level of MPM-2 detectable phosphorylation was still significantly lower in DAP5-deficient cells (Figure 7B).

Among the substrates of the CDK1/cyclin B complex is survivin, an M phase-specific inhibitor of apoptosis (IAP), which is stabilized following phosphorylation on Thr34 by CDK1 at the onset of mitosis (Andersen and thor Straten, 2002; Li et al., 1998; Li and Ling, 2006; O'Connor et al., 2000, 2002). Therefore, we measured the steady-state levels of survivin in DAP5-depleted HeLa cells following taxol treatment as another indirect reflection of the status of CDK1 activity in cells. Significantly, knockdown of DAP5 resulted in reduced steady-state levels of the endogenous survivin and this effect persisted in the presence of zVAD (Figure 7C). This implies that DAP5 is required for the stabilization of survivin during mitosis, probably by modulating CDK1 translation and consequently reducing its overall cellular activity. These data provide additional confirmation that defective translation of CDK1 due to the loss of DAP5 has a major impact upon its cellular function.

#### DISCUSSION

In this manuscript, we report on a mechanism by which DAP5, a mediator of cap-independent translation, impacts on cell

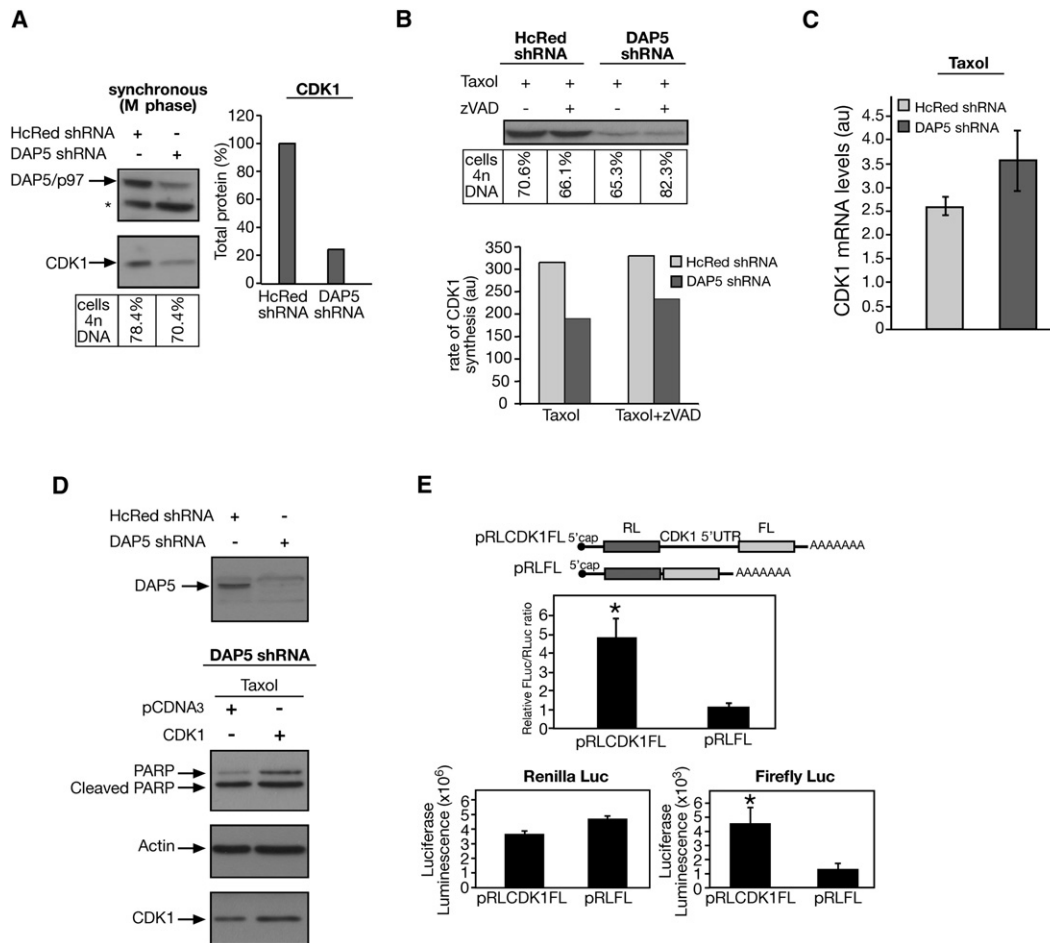


**Figure 6. Depletion of DAP5 by shRNA Affects Translation of CDK1 during Mitosis**

(A) HeLa cells were transiently transfected with shRNA against DAP5 or HcRed for 5 days and then synchronized by double thymidine block. Cells were collected 8 hr following the release from the second block. Western blot was performed with the indicated antibodies. Asterisk represents nonspecific band. Graph represents quantification of the signal by densitometry analysis; the HcRed signal was set as 100%.

(B) HeLa cells were depleted of DAP5 as in (A) and treated with taxol in the presence or absence of zVAD for 16 hr, and then metabolically labeled with  $^{35}\text{S}$ -Met. Cell extracts were prepared, and equal amounts of radioactivity ( $5 \times 10^7$  CPM) were subjected to immunoprecipitation with anti-CDK1 antibodies. The immunoprecipitates were separated on SDS-PAGE, and signal intensities were quantified by densitometry using the BAS-2000 PhosphorImager (Fuji) and ProbeQuant software (Fuji) (graph). Western blot was used to determine efficient knockdown of DAP5, and the percent of cells with 4n DNA content was determined by FACS analysis (top).

(C) Total RNA was isolated from taxol-treated HeLa cells depleted of DAP5 and was converted to cDNA. The cDNA was subjected to real-time PCR. Relative amounts of CDK1 mRNA in each sample normalized to HPRT mRNA are presented as the mean  $\pm$  SD of triplicates. The experiment was repeated three times with reproducible results.

(D) HeLa cells were transfected with DAP5 shRNA for 48 hr and then transfected with pCDNA3 plasmid or CDK1 plasmid, as detailed in the *Experimental Procedures*. Cells were then treated with taxol for 16 hr. (Top) Representative western blot of DAP5 decrease in this experiment. (Bottom) Western blot of PARP-1, actin, and CDK1. The rescue experiment was repeated several times with reproducible results.

(E) HeLa cells were transfected with in vitro-transcribed mRNA corresponding to pRLCDK1FL or pRLFL. Luciferase activity was analyzed 6 hr following the transfection. (Top) Schematic representation of pRLCDK1FL and pRLFL mRNA transcripts. The pRLFL vector contains a linker of 100 bp instead of the IRES element. (Bottom) Upper graph represents relative luciferase activity (ratio of firefly/renilla). The average activity in the control vector has been designated as 1. Lower graphs represent the absolute values reflecting renilla and firefly luciferase activity, separately, for each transcript. The values represent the mean  $\pm$  SD of triplicates. The experiment was repeated three times with reproducible results. Asterisks mark a statistically significant result ( $p < 0.01$ ).

survival. Knockdown of DAP5 from cells by RNA interference results in substantial loss of cell viability, in particular during the mitotic phase, via activation of caspase-dependent pathways. The molecular basis for this apoptotic phenotype is provided here by identifying two mRNA targets, Bcl-2 and CDK1, the translation of which is modulated by DAP5.

Several findings on the mode of action of DAP5, shown here in unstressed cells, emphasize the issue of selectivity toward cap-independent translation. We find that depletion of DAP5 by itself does not direct the disassembly of polysomes in cells, and that actin mRNA chosen as a representative target driven by cap-dependent translation remains in heavy polysomes. In contrast,

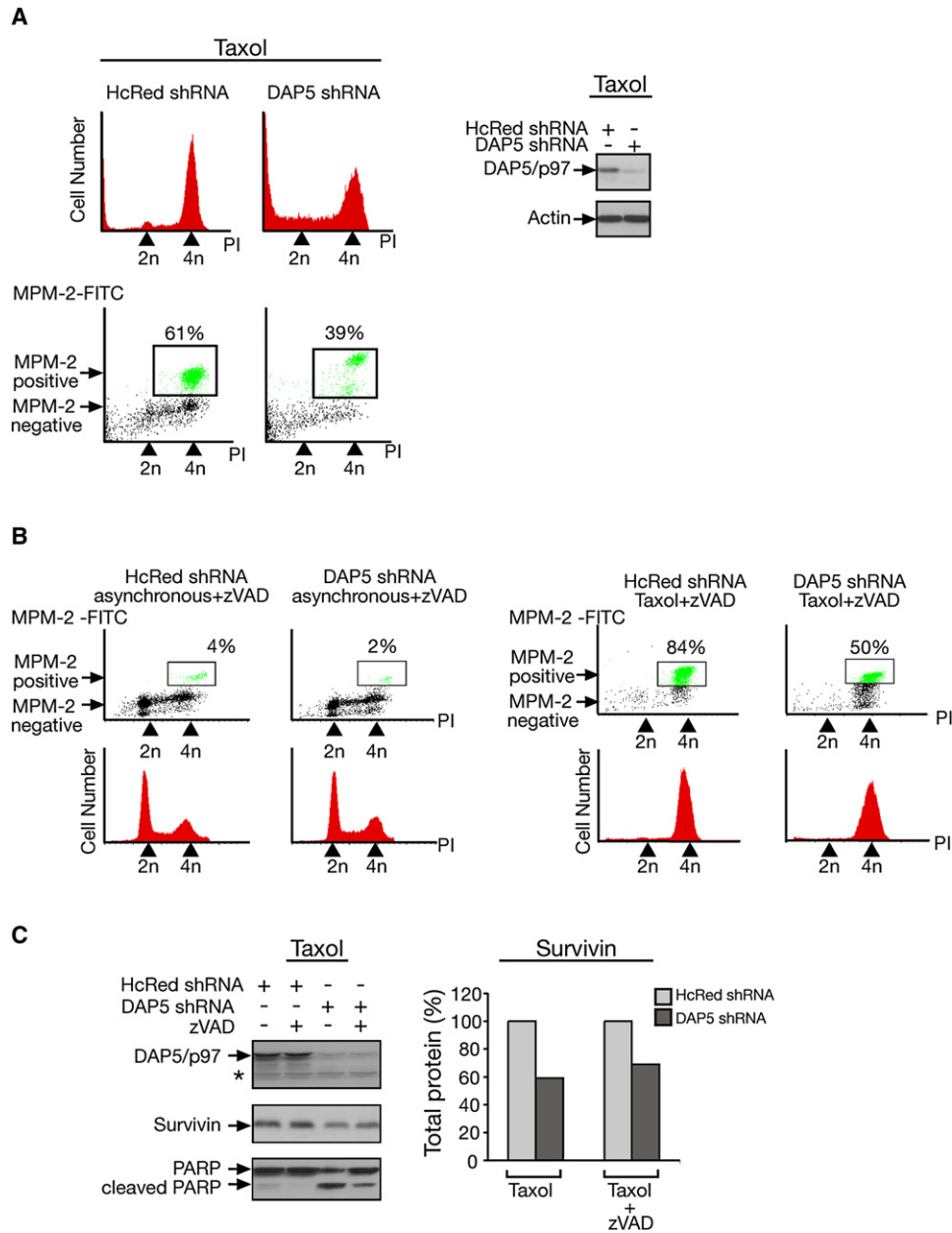


**Figure 7. DAP5 Knockdown Cells Display a Decline in CDK1-Mediated Substrate Phosphorylation during Mitosis**

(A) FACS analysis of DAP5-depleted cells versus control cells stained with MPM-2 antibodies. Cells transfected with shRNA against DAP5 or HcRed for 5 days were treated with taxol for 16 hr and stained with MPM-2 antibodies. The same samples were further stained for DNA content with propidium iodide and analyzed by flow cytometry. MPM-2 and PI staining were detected as FITC and PE fluorescence, respectively. (Left) Histograms represent cell-cycle distribution of  $10^5$  cells according to DNA content. Dot plots represent MPM-2 staining (y axis, logarithmic scale) along the cell cycle (x axis). MPM-2-positive cells are gated, and percentages are indicated. (Right) Western blot for DAP5 represents the efficiency of RNA interference.

(B) Cells were treated for 16 hr with taxol (or DMSO as control) in the presence of zVAD and were stained with MPM-2 antibodies as in (A). (Left) FACS analysis for MPM-2 staining and DNA content on exponentially growing (asynchronous) cells. (Right) FACS analysis for MPM-2 staining and DNA content on taxol-treated cells. MPM-2-positive populations are gated, and percentages are indicated.

(C) Cells were treated with taxol in the presence or absence of zVAD for 16 hr. Steady-state levels of indicated proteins were assessed by immunoblotting. Graph represents relative quantification of the survivin signals by densitometric analysis.

Bcl-2 mRNA, found to be a direct mRNA target of DAP5, shifts toward light and subpolysomal fractions reflecting its reduced efficiency of translation initiation in response to DAP5 depletion.

Furthermore, a direct functional measurement of the Bcl-2 IRES expressed from a bicistronic vector proves the exclusive dependence of this type of cap-independent translation on the

presence of DAP5. Thus, we provide mechanistic insight concerning the mode of action of DAP5 as a translation factor in cycling unstressed cells.

The identification of CDK1 as a second target of DAP5 and the work that followed this discovery highlighted the important role that DAP5 has in driving the cap-independent initiation during mitosis. In fact, these data demonstrate the existence of an additional layer of regulation of CDK1 expression during mitosis, on top of the well-studied posttranslational modifications that serve to regulate the kinase activity (Doree and Hunt, 2002; Schafer, 1998; Stark and Taylor, 2006). Impaired translation of CDK1 during mitosis in DAP5-deficient cells resulted in a significant decrease in the phosphorylation of its target proteins within cells, indicating that de novo synthesis of CDK1 during mitosis is critical for its cellular functions and for maintaining cell survival during mitosis. Notably, entry into mitosis was not affected by DAP5 knockdown, suggesting that each cellular outcome (i.e., G2 to M phase progression versus cell survival during mitosis) relies on a different threshold of the active CDK1 kinase. The newly synthesized molecules during mitosis that are regulated by DAP5 may have a functional advantage over the pre-existing CDK1 in which inhibitory phosphorylations need to be removed for the kinase to be activated.

It is not clear whether and how the activity of DAP5 is regulated along the cell cycle. To date, proteolytic cleavage by caspases into the 86 kDa protein (DAP5/p86) was proposed as one of the mechanisms activating DAP5's translation function in responses to various stress signals (Henis-Korenblit et al., 2000; Marash and Kimchi, 2005). The findings presented here strongly indicate that the full-length DAP5/p97 is a positive regulator of cap-independent translation in unstressed cells. It is possible that specific posttranslational modifications other than proteolytic cleavage modulate DAP5/p97 activity in a cell-cycle-dependent manner.

Notably, the mitotic cell death that develops in response to DAP5 knockdown is caspase dependent and can be partially rescued by the ectopic expression of Bcl-2 or CDK1. The central role of Bcl-2 in regulating cell survival has been extensively discussed in numerous publications. (Burlacu, 2003; Kelekar and Thompson, 1998; Kim, 2005; Willis et al., 2003). Specifically, its functional contribution to cell survival at the mitotic phase has also been addressed. It was found in this respect that microtubule-targeting drugs such as taxol cause a reduction in the Bcl-2/Bax ratio that below a certain threshold can drive the cells toward apoptosis. In addition, inhibition of Bcl-2 expression by antisense oligonucleotides was shown to facilitate and amplify a process called "mitotic catastrophe," a type of cell death occurring during mitosis or resulting from mitotic failure (Castedo et al., 2004). Therefore, Bcl-2 may also act during mitosis as a guardian of microtubule integrity (Basu and Haldar, 1998; Castedo et al., 2004). The contribution of CDK1 to the cell-death process is consistent with previous reports that applied Purvalanol A, a CDK1 kinase inhibitor, to HeLa cells arrested in mitosis by taxol (O'Connor et al., 2002). The CDK1 inhibitory drug caused the destabilization of survivin protein and subsequent loss of cell viability at the mitotic phase similar to the effect of DAP5 knockdown shown here. In addition, it was recently published that caspase-9 is phosphorylated at Thr125 during mitosis by

CDK1 and that this phosphorylation is important in maintaining cell survival during mitosis (Allan and Clarke, 2007). Thus, the phosphorylation of survivin and of caspase-9 during mitosis supports the concept that CDK1 restrains apoptosis during mitosis. Future work may reveal additional CDK1-mediated phosphorylation events that are cell death protective, as well as additional unknown yet DAP5 targets, other than Bcl-2 and CDK1, which may also be involved in this caspase-dependent M phase-specific cell death.

The identification of two key regulators of cell survival, CDK1 and Bcl-2, as translation targets of DAP5 strongly implies that DAP5 might be involved in carcinogenesis. Moreover, the ability of shRNA-targeting DAP5 to sensitize human cancer cells treated with the anticancer drug taxol to apoptosis indicates that DAP5 has an excellent potential to serve as a target for anticancer therapy in the future.

## EXPERIMENTAL PROCEDURES

### Cell Cultures, Synchronization Procedures, Viability Assays, and Chemical Inhibitors

The HeLa human cervical carcinoma and HEK293T cell lines were grown in Dulbecco's modified Eagle's medium (Biological Industries, Beit Haemek, Israel), supplemented with 10% fetal bovine serum (Hyclone), 4 mM glutamine (GIBCOBRL), and antibiotics (GIBCOBRL). Cells were synchronized at the G1/S boundary by double thymidine block (2 mM thymidine, Sigma) for 14 hr each time, separated by a 9 hr release. For single thymidine block, HeLa cells were grown for 16 hr in the presence of 2 mM thymidine. For M phase arrest, the cells were grown for 16 hr in the presence of 0.2  $\mu$ M taxol (Paclitaxel, Sigma). For the trypan blue assays, floating and attached cells were collected and cell death was measured by uptake of trypan blue (Sigma) into cells that had lost membrane integrity. The broad caspase inhibitor zVAD-fmk (Sigma) was used at the final concentration of 50  $\mu$ M for 16–24 hr, as indicated. Proteasome inhibitor MG132 (Calbiochem) was used at a final concentration of 10  $\mu$ M for 16 hr or 100  $\mu$ M for 6 hr.

### siRNA and Rescue Experiments

siGENOME SMARTpool siRNA against DAP5 (eIF4G2), siCONTROL nontargeting siRNA #1 (Dharmacon), or siRNA against HcRed was introduced into HeLa cells using the Transit-LT1+Transit-TKO transfection kits (Mirus), according to the manufacturer's instructions or by the standard calcium-phosphate precipitation method. Bcl-2 rescue experiments were as follows: HeLa cells were cotransfected with DAP5 shRNA and pCDNA3 (Invitrogen) or Bcl-2 (NM\_000633.2, ORIGENE) (5  $\mu$ g per 9 cm plate). Transfection was performed by the standard calcium-phosphate precipitation method. Following 5 days of transfection, cells were treated with DMSO or taxol for 16 hr. CDK1 rescue experiments were as follows: HeLa cells were transfected with DAP5 shRNA for 48 hr and then transfected with pCDNA3 (Invitrogen) or CDK1 (15  $\mu$ g per 9 cm plate) (NM\_001786.2, ORIGENE). Transfections were performed by the standard calcium-phosphate precipitation method. Following 24 hr of second transfection, cells were treated with taxol for 16 hr. DNA expression vectors and transfection procedures are provided in the [Supplemental Data](#).

### Protein Analysis

Cells were lysed in B buffer or in PLB buffer supplemented with a mixture of protease and phosphatase inhibitors (Supplemental Data). For immunoprecipitations, 2–5 mg of precleared total protein extracts was incubated with the relevant antibody pre-conjugated to Protein G or A agarose beads (Santa Cruz). Immunoprecipitates or total cell lysates (10–100  $\mu$ g) were separated on 10%–15% SDS-PAGE and western blotted with specific antibodies (Supplemental Data). Densitometry analysis of protein bands was performed using ImageJ software.

### Metabolic Labeling

HeLa cells were incubated with DMEM depleted of methionine (Biological Industries, Beit-Hamek) for 1 hr and then labeled with 80  $\mu\text{Ci/ml}$   $^{35}\text{S}$ -Met (Amersham) for 30 min. For overall translation rate measurement, samples were subjected to TCA precipitation (Sigma). The level of TCA insoluble radioactivity was detected by  $\beta$  counter scintillation and calculated per microgram total protein. For rate of synthesis of individual proteins, samples of protein extracts corresponding to  $5 \times 10^9$ – $10^7$  CPM were subjected to immunoprecipitation with the relevant antibodies. Signal intensities were determined by densitometry using the BAS-2000 PhosphorImager (Fuji) and ProbeQuant software (Fuji).

### Protein-mRNA Coimmunoprecipitation

293T cells were harvested, and 5 mg of precleared protein extracts was immunoprecipitated with Protein G agarose-bound M2-Flag antibodies (Sigma) or anti-DAP5 antibodies for 2 hr at 4°C. The beads were subsequently washed, resuspended, and incubated for 30 min at 55°C with 30  $\mu\text{g}$  Proteinase K. The population of coimmunoprecipitated mRNA was isolated using standard phenol-chloroform extraction and ethanol precipitation in the presence of glycogen (Roche) as a carrier. Additional details are provided in the [Supplemental Data](#).

### cDNA Array Analysis

Single-stranded cDNA, limited by an adaptor sequence at both ends, was produced by the Super SMART cDNA synthesis kit (Clontech) according to the recommended procedure, using anti-Flag immunoprecipitated mRNA from Flag-DAP5/p86 or control transfectants as template. Upon removal of unincorporated primers and nucleotides by column chromatography, the ss-cDNA served as a template for Long Distance PCR (Clontech), according to the manufacturer's instructions. To produce radiolabeled probe, the amplified PCR products were incubated with a primer mixture corresponding to the 200 genes represented on the Human Panorama Apoptosis Array (Sigma), dNTPs, [ $\alpha$ - $^{32}\text{P}$ ]dATP (Amersham), labeling buffer, and Klenow polymerase (Sigma), using the recommended protocol. Finally, the purified radiolabeled probes were hybridized overnight in ExpressHyb Hybridization Solution (Clontech) to a Human Panorama Apoptosis Array (Sigma) that had been preincubated with the SMART Blocking Solution (Clontech). After several washes, the cDNA arrays were scanned with a BAS-2000 PhosphorImager (Fuji) and were then analyzed using ProbeQuant software (Fuji). A default background setting was determined by membrane slots spotted with TE or with irrelevant DNA. These were used in conjunction with a signal minus local background threshold to exclude insignificant gene signal intensities. An average of all housekeeping gene signals on the array (assumed not to be DAP5 targets) was used to normalize the signal intensity between array pairs. Changes in the mRNA profile of Flag-DAP5/p86 mRNP complexes in comparison to control immunoprecipitates were considered significant if they were 2-fold or greater.

### In Vitro Transcription, RNA Transfections, and Reporter Assay

Capped mRNA transcripts were produced using the T7 Message Machine kit (Ambion) on DNA constructs linearized with AgeI (Bcl-2 bicistronic constructs) or XhoI (CDK1 bicistronic constructs) and recovered according to the manufacturer's instructions. CDK1 bicistronic transcripts were then in vitro polyadenylated using an RNA Polyadenylation kit (Ambion). Final recovery of RNA transcripts was achieved with the MEGAclear kit (Ambion). Corresponding mRNAs were introduced into HeLa cells using TransMessenger Transfection Reagent (QIAGEN) according to the manufacturer's instructions. Cells were washed 3 hr following transfection. Luciferase activity was measured with a Veritas Microplate Luminometer (Promega) 6 hr after transfection (Sherrill et al., 2004; Yoon et al., 2006) using the Dual-Luciferase Reporter Assay System (Promega), according to the manufacturer's protocol.

### Polysomal Profile Analysis and Real-Time PCR from Sucrose Gradient Fractions

Polysomal profiles were performed as described in Sivan et al. (2007). Equal volumes from each of fractions 13–23 and from a pool of fractions 6–12 (termed "subpolysomes") were used to perform RT-PCR followed by real-time PCR as described in the [Supplemental Data](#).

### Flow Cytometry Analysis

Attached and floating HeLa cells were collected and fixed in 70% ethanol in PBS. For DNA content analysis, the cells were stained with 40  $\mu\text{g/ml}$  propidium iodide (Sigma) and 1 mg/ml RNase A (Sigma). For staining with MPM-2 antibodies, ethanol-fixed cells were permeabilized with 0.25% Triton X-100 and subsequently stained with 6  $\mu\text{g/ml}$  mouse monoclonal MPM-2 antibody (Upstate). FITC-conjugated donkey anti-mouse IgG (Jackson ImmunoResearch) was used as a secondary antibody. The cells were stained for DNA content with 5  $\mu\text{g/ml}$  propidium iodide (Sigma) in the presence of 200  $\mu\text{g/ml}$  RNase A (Sigma). Samples were then analyzed by a FACSort cytometer (Becton Dickinson), using an excitation laser of 488 nm and emission filter of 530/30 nm (FITC) or emission filter of 585/42 nm (PI).

### Statistical Analysis

The data were expressed as mean  $\pm$  SD. Statistical significance was determined using Student's *t* test (two-tailed). The criterion for statistical significance was considered  $p < 0.05$ .

### SUPPLEMENTAL DATA

Supplemental Data include six figures, Supplemental Experimental Procedures, and Supplemental References and can be found with this article online at <http://www.molecule.org/cgi/content/full/30/4/447/DC1/>.

### ACKNOWLEDGMENTS

We thank R. Lloyd for providing the bicistronic constructs with Bcl-2 IRES. We thank Dr. S. Bialik for critical reading of this manuscript, Dr. A. Gamliel for generating the DAP5 shRNA construct, E. Zalckvar for generating the HcRed shRNA construct, and A. Sharp for the assistance with FACS analysis. This work was supported by the Center of Excellence grant from the Flight Attendant Medical Research Institute (FAMRI) to A.K., the Kahn Fund for System Biology at the Weizmann Institute of Science to A.K., and by a grant from the Israel Science Foundation (to O.E.-S.). A.K. is the incumbent of Helena Rubinstein Chair of Cancer Research.

Received: May 30, 2007

Revised: January 9, 2008

Accepted: March 7, 2008

Published online: May 1, 2008

### REFERENCES

- Allan, L.A., and Clarke, P.R. (2007). Phosphorylation of caspase-9 by CDK1/cyclin B1 protects mitotic cells against apoptosis. *Mol. Cell* 26, 301–310.
- Andersen, M.H., and Thor Straten, P. (2002). Survivin—a universal tumor antigen. *Histol. Histopathol.* 17, 669–675.
- Basu, A., and Haldar, S. (1998). The relationship between Bcl2, Bax and p53: consequences for cell cycle progression and cell death. *Mol. Hum. Reprod.* 4, 1099–1109.
- Burlacu, A. (2003). Regulation of apoptosis by Bcl-2 family proteins. *J. Cell. Mol. Med.* 7, 249–257.
- Castedo, M., Perfettini, J.L., Roumier, T., Andreau, K., Medema, R., and Kroemer, G. (2004). Cell death by mitotic catastrophe: a molecular definition. *Oncogene* 23, 2825–2837.
- Cornelis, S., Bruynooghe, Y., Denecker, G., Van Huffel, S., Tinton, S., and Beyaert, R. (2000). Identification and characterization of a novel cell cycle-regulated internal ribosome entry site. *Mol. Cell* 5, 597–605.
- Doree, M., and Hunt, T. (2002). From Cdc2 to Cdk1: when did the cell cycle kinase join its cyclin partner? *J. Cell Sci.* 115, 2461–2464.
- Eiroy-Stein, O., and Merrick, W.C. (2007). Translation initiation via cellular internal ribosome entry sites. In *Translational Control in Biology and Medicine*, M.B. Mathews, N. Sonenberg, and J.W.B. Hershey, eds. (Cold Spring Harbor, NY: Cold Spring Harbor Laboratory Press), pp. 155–172.

- Henis-Korenblit, S., Strumpf, N.L., Goldstau, D., and Kimchi, A. (2000). A novel form of DAP5 protein accumulates in apoptotic cells as a result of caspase cleavage and internal ribosome entry site-mediated translation. *Mol. Cell. Biol.* 20, 496–506.
- Henis-Korenblit, S., Shani, G., Sines, T., Marash, L., Shohat, G., and Kimchi, A. (2002). The caspase-cleaved DAP5 protein supports internal ribosome entry site-mediated translation of death proteins. *Proc. Natl. Acad. Sci. USA* 99, 5400–5405.
- Hundsdoerfer, P., Thoma, C., and Hentze, M.W. (2005). Eukaryotic translation initiation factor 4G1 and p97 promote cellular internal ribosome entry sequence-driven translation. *Proc. Natl. Acad. Sci. USA* 102, 13421–13426.
- Imataka, H., Olsen, H.S., and Sonenberg, N. (1997). A new translational regulator with homology to eukaryotic translation initiation factor 4G. *EMBO J.* 16, 817–825.
- Jackson, R.J. (2005). Alternative mechanisms of initiating translation of mammalian mRNAs. *Biochem. Soc. Trans.* 33, 1231–1241.
- Keene, J.D. (2001). Ribonucleoprotein infrastructure regulating the flow of genetic information between the genome and the proteome. *Proc. Natl. Acad. Sci. USA* 98, 7018–7024.
- Kelekar, A., and Thompson, C.B. (1998). Bcl-2-family proteins: the role of the BH3 domain in apoptosis. *Trends Cell Biol.* 8, 324–330.
- Kim, R. (2005). Unknotting the roles of Bcl-2 and Bcl-xL in cell death. *Biochem. Biophys. Res. Commun.* 333, 336–343.
- Le Breton, M., Cormier, P., Belle, R., Mulner-Lorillon, O., and Morales, J. (2005). Translational control during mitosis. *Biochimie* 87, 805–811.
- Lee, S.H., and McCormick, F. (2006). p97/DAP5 is a ribosome-associated factor that facilitates protein synthesis and cell proliferation by modulating the synthesis of cell cycle proteins. *EMBO J.* 25, 4008–4019.
- Levy-Strumpf, N., Deiss, L.P., Berissi, H., and Kimchi, A. (1997). DAP-5, a novel homolog of eukaryotic translation initiation factor 4G isolated as a putative modulator of gamma interferon-induced programmed cell death. *Mol. Cell. Biol.* 17, 1615–1625.
- Lewis, S.M., Cerquozzi, S., Graber, T.E., Ungureanu, N.H., Andrews, M., and Holcik, M. (2008). The eIF4G homolog DAP5/p97 supports the translation of select mRNAs during endoplasmic reticulum stress. *Nucleic Acids Res.* 36, 168–178.
- Li, F., and Ling, X. (2006). Survivin study: an update of “what is the next wave”? *J. Cell. Physiol.* 208, 476–486.
- Li, F., Ambrosini, G., Chu, E.Y., Plescia, J., Tognin, S., Marchisio, P.C., and Altieri, D.C. (1998). Control of apoptosis and mitotic spindle checkpoint by survivin. *Nature* 396, 580–584.
- Marash, L., and Kimchi, A. (2005). DAP5 and IRES-mediated translation during programmed cell death. *Cell Death Differ.* 12, 554–562.
- Nevins, T.A., Harder, Z.M., Korneluk, R.G., and Holcik, M. (2003). Distinct regulation of internal ribosome entry site-mediated translation following cellular stress is mediated by apoptotic fragments of eIF4G translation initiation factor family members eIF4G1 and p97/DAP5/NAT1. *J. Biol. Chem.* 278, 3572–3579.
- Nousch, M., Reed, V., Bryson-Richardson, R.J., Currie, P.D., and Preiss, T. (2007). The eIF4G-homolog p97 can activate translation independent of caspase cleavage. *RNA* 13, 374–384.
- O'Connor, D.S., Grossman, D., Plescia, J., Li, F., Zhang, H., Villa, A., Tognin, S., Marchisio, P.C., and Altieri, D.C. (2000). Regulation of apoptosis at cell division by p34cdc2 phosphorylation of survivin. *Proc. Natl. Acad. Sci. USA* 97, 13103–13107.
- O'Connor, D.S., Wall, N.R., Porter, A.C., and Altieri, D.C. (2002). A p34(cdc2) survival checkpoint in cancer. *Cancer Cell* 2, 43–54.
- Prevot, D., Darlix, J.L., and Ohlmann, T. (2003). Conducting the initiation of protein synthesis: the role of eIF4G. *Biol. Cell* 95, 141–156.
- Pyronnet, S., and Sonenberg, N. (2001). Cell-cycle-dependent translational control. *Curr. Opin. Genet. Dev.* 11, 13–18.
- Pyronnet, S., Pradayrol, L., and Sonenberg, N. (2000). A cell cycle-dependent internal ribosome entry site. *Mol. Cell* 5, 607–616.
- Schafer, K.A. (1998). The cell cycle: a review. *Vet. Pathol.* 35, 461–478.
- Shaughnessy, J.D., Jr., Jenkins, N.A., and Copeland, N.G. (1997). cDNA cloning, expression analysis, and chromosomal localization of a gene with high homology to wheat eIF-(iso)4F and mammalian eIF-4G. *Genomics* 39, 192–197.
- Sherrill, K.W., Byrd, M.P., Van Eden, M.E., and Lloyd, R.E. (2004). BCL-2 translation is mediated via internal ribosome entry during cell stress. *J. Biol. Chem.* 279, 29066–29074.
- Sivan, G., Kedersha, N., and Elroy-Stein, O. (2007). Ribosomal slowdown mediates translational arrest during cellular division. *Mol. Cell. Biol.* 27, 6639–6646.
- Spriggs, K.A., Bushell, M., Mitchell, S.A., and Willis, A.E. (2005). Internal ribosome entry segment-mediated translation during apoptosis: the role of IRES-trans-acting factors. *Cell Death Differ.* 12, 585–591.
- Stark, G.R., and Taylor, W.R. (2006). Control of the G2/M transition. *Mol. Biotechnol.* 32, 227–248.
- Tenenbaum, S.A., Carson, C.C., Lager, P.J., and Keene, J.D. (2000). Identifying mRNA subsets in messenger ribonucleoprotein complexes by using cDNA arrays. *Proc. Natl. Acad. Sci. USA* 97, 14085–14090.
- Tenenbaum, S.A., Lager, P.J., Carson, C.C., and Keene, J.D. (2002). Ribonucleic acids: identifying mRNA subsets in mRNP complexes using antibodies to RNA-binding proteins and genomic arrays. *Methods* 26, 191–198.
- Warnakulasuriyarachchi, D., Cerquozzi, S., Cheung, H.H., and Holcik, M. (2004). Translational induction of the inhibitor of apoptosis protein HIAP2 during endoplasmic reticulum stress attenuates cell death and is mediated via an inducible internal ribosome entry site element. *J. Biol. Chem.* 279, 17148–17157.
- Willis, S., Day, C.L., Hinds, M.G., and Huang, D.C. (2003). The Bcl-2-regulated apoptotic pathway. *J. Cell Sci.* 116, 4053–4056.
- Yamanaka, S., Poksay, K.S., Arnold, K.S., and Innerarity, T.L. (1997). A novel translational repressor mRNA is edited extensively in livers containing tumors caused by the transgene expression of the apoB mRNA-editing enzyme. *Genes Dev.* 11, 321–333.
- Yamanaka, S., Zhang, X.Y., Maeda, M., Miura, K., Wang, S., Farese, R.V., Jr., Iwao, H., and Innerarity, T.L. (2000). Essential role of NAT1/p97/DAP5 in embryonic differentiation and the retinoic acid pathway. *EMBO J.* 19, 5533–5541.
- Yoon, A., Peng, G., Brandenburger, Y., Zollo, O., Xu, W., Rego, E., and Ruggero, D. (2006). Impaired control of IRES-mediated translation in X-linked dyskeratosis congenita. *Science* 312, 902–906.
- Yoshikane, N., Nakamura, N., Ueda, R., Ueno, N., Yamanaka, S., and Nakamura, M. (2007). Drosophila NAT1, a homolog of the vertebrate translational regulator NAT1/DAP5/p97, is required for embryonic germband extension and metamorphosis. *Dev. Growth Differ.* 49, 623–634.